Equilibrium Shapes of Erythrocytes in Rouleau Formation

Jure Derganc,* Bojan Božič,* Saša Svetina,*† and Boštjan Žekš*†
*Institute of Biophysics, Faculty of Medicine, University of Ljubljana, Lipičeva 2, SI-1000 Ljubljana, Slovenia and †J. Stefan Institute, Jamova 39, SI-1111 Ljubljana, Slovenia

ABSTRACT A well known physiological property of erythrocytes is that they can aggregate and form a rouleau. We present a theoretical analysis of erythrocyte shapes in a long rouleau composed of cells with identical sizes. The study is based on the area difference elasticity model of lipid membranes, and takes into consideration the adhesion of curved axisymmetric membranes. The analysis predicts that the erythrocytes in the rouleau can have either a discoid or a cup-like shape. These shapes are analogous to the discoid and stomatocyte shapes of free erythrocytes. The transitions between the discoid and cup-like shapes in the rouleau are characterized. The occurrence of these transitions depends on three model parameters: the cell relative volume, the preferred difference between the areas of the membrane bilayer leaflets, and the strength of the adhesion between the membranes. The cup-like shapes are favored at small relative volumes and small preferred area differences, and the discoid shapes are favored at large values of these parameters. Increased adhesion strength enlarges the contact area between the cells, flattens the cells, and consequently promotes the discoid shapes.

INTRODUCTION

Erythrocytes in low shear flow can aggregate and form a close packed stack of cells, the so-called *rouleau*. Although the rouleau formation has now been known for more than a hundred years and has been thoroughly investigated, it still attracts considerable research interest. The reason for its importance is at least twofold. From the clinical point of view, erythrocyte aggregation is interesting because it can significantly influence blood viscosity in vivo (Bishop et al., 2001). For example, some hemorheological abnormalities which occur in patients suffering from diabetes mellitus can be related to increased rouleau formation (Candiloros et al., 1996). In addition, aggregating erythrocytes provide a well controlled model system for basic research in various biophysical fields. For example, rouleau formation has been used in studies of the general properties of membrane-membrane interactions (Darmani and Coakley, 1990), and in studies of dextran polymer conformation (Barshtein et al., 1998).

To fully understand rouleau formation, a thorough theoretical analysis of the mechanics involved in the process is clearly necessary. A basic treatment of the mechanics of rouleau formation has been given by Skalak et al. (1981). It was recognized that the process is governed by an interplay of intercellular adhesion, which drives the aggregation, and erythrocyte mechanical rigidity. The authors developed a model of rouleau formation based on the erythrocyte membrane bending and shear elasticities, and were able to relate the equilibrium shape of erythrocytes in the rouleau to the strength of the intercellular adhesion. They found that the adhesion energy between normal aggregated erythrocytes was of the order of 10^{-19} $J / \mu m^2$. In their subsequent work (Skalak and Chien, 1983; Chien et al., 1983), the analysis was brought even further by using experiments in which the adhesion strength was controlled by the concentration of dextran polymers in the solution.

The approach used by Skalak et al. (1981) considered aggregating erythrocytes with flat contact surfaces, and accordingly only the cell shape geometries possessing equatorial mirror symmetry. Their analysis covered a large part of the observed behavior, however erythrocyte aggregates with curved contact surfaces can exist as well. Indeed, electron micrographs show rouleau formations comprised of cup-shaped erythrocytes with curved contact surfaces (see, for example, Darmani and Coakley, 1990; and Chien et al., 1983). In fact, inasmuch as the free erythrocytes can exist as both mirror-symmetric discocytes and cup-shaped stomatocytes, it is likely that adhering erythrocytes possess analogous properties.

The aim of the present paper is to give a theoretical analysis which covers all possible axisymmetric equilibrium shapes of erythrocytes in a long rouleau composed of identical cells. Thus, the stomatocyte-like shapes, i.e., shapes without equatorial mirror symmetry, are considered as well. The analysis is based on the computational approaches developed in the study of lipid membranes (Božič et al., 1997). Therefore the study further extends the work of Skalak et al. (1981) also by taking into account the bilayer nature of erythrocyte lipid membrane.

THEORY

Energy of erythrocytes in rouleau

To aggregate into a rouleau, the erythrocytes have to deform from their normal biconcave shape. Accordingly, the equilibrium state of erythrocytes in the rouleau corresponds to the minimum of the sum of the adhesion energy and the elastic energy of their membrane (Skalak et al., 1981).

Erythrocyte mechanical properties arise from the elastic properties of its lipid bilayer and the underlying membrane skeleton. The membrane skeleton

Submitted June 20, 2002, and accepted for publication October 18, 2002.
Address reprint requests to Jure Derganc, Institute of Biophysics, Lipiceva 2, Ljubljana, Slovenia 1000. Tel.: 286-1-543-7600; Fax: 386-1-431-5127; E-mail: jure.derganc@biofiz.mf.uni-lj.si.

0006-3495/03/03/1486/07 $2.00

elasticity is believed to be important at large cell deformations which occur for example in high shear flow or in echinocyte transformation. Deformations of erythrocytes in the rouleau formation are much smaller, therefore the skeleton elasticity can be safely omitted from the analysis. Indeed, the computation of the mirror symmetric shapes over a wide range of the membrane skeleton shear constant yielded qualitatively similar results (Skalak and Chien, 1983). Thus, the main energy terms of the rouleau formation can be assumed to be the elastic energy of the membrane bilayer and the intercellular adhesion energy.

The elastic properties of closed lipid bilayers are well described by the *area difference elasticity* (ADE) model (Božič et al., 1992; Miao et al., 1994) (this model is also called the *generalized bilayer couple* model). The cell membrane energy within the ADE model is the sum of the membrane bending energy and the nonlocal bending energy:

$$W_{\mathrm{el}} = \frac{k_{\mathrm{c}}}{2}\int (C_1 + C_2 - C_0)^2\, dA + \frac{k_{\mathrm{r}}}{2Ah^2}(\Delta A - \Delta A_0)^2, \quad (1)$$

where k_{c} is the local bending modulus, C_1 and C_2 are the membrane principal curvatures, C_0 is the membrane spontaneous curvature, k_{r} is the nonlocal bending modulus, A is the cell surface area, h is the separation distance between the neutral surfaces of the two leaflets of the bilayer, ΔA is the difference in the areas of the two leaflets of the bilayer, and ΔA_0 is the area difference between the leaflets when both leaflets are stress-free. The value of ΔA_0 is directly related to the difference in the number of molecules in the membrane leaflets. It turns out that at given bending moduli, the spontaneous curvature C_0 and the preferred area difference ΔA_0 can be combined into a single parameter, denoted the effective preferred area difference $\overline{\Delta A}_0 = \Delta A_0 + (k_{\mathrm{c}}/k_{\mathrm{r}})\, hAC_0$, without losing the generality of the model (Svetina et al., 1985; Miao et al., 1994).

The interactions which drive erythrocyte aggregation are not known in detail, but one can assume that the effective intercellular interaction is constant and uniform over the contact surface (Skalak et al., 1981). Therefore, the adhesion energy of an erythrocyte is proportional to the strength of the effective intercellular interaction and the area of the contact surface:

$$W_{\mathrm{adh}} = -\gamma A_{\mathrm{c}}, \quad (2)$$

where γ is the effective adhesion constant and A_{c} is the erythrocyte contact surface area. Note that in a long rouleau, two adjacent erythrocytes share the same contact surface area and therefore the adhesion energy *per* cell is one half of W_{adh}. The analysis can be conveniently carried out by using the dimensionless variables rescaled with respect to a spherical cell with a unity surface area. The unit of length in this representation is $R_0 = \sqrt{A/4\pi}$, and the unit of energy is the bending energy of a spherical membrane, $W_{\mathrm{sphere}} = 8\pi k_{\mathrm{c}}$. Within this normalization, a cell with a volume V and a surface area A is characterized by only one parameter – the relative volume which is defined as $v = V/\left((4/3)\pi R_0^3\right)$. The total energy *per* erythrocyte in a rouleau, $W = W_{\mathrm{el}} + (1/2)W_{\mathrm{adh}}$, is thus written in the dimensionless form as:

$$w = \frac{1}{4}\int (c_1 + c_2)^2\, da + q(\Delta a - \overline{\Delta a}_0)^2 - \frac{1}{2}\bar{\gamma} a_{\mathrm{c}}, \quad (3)$$

where the dimensionless variables are defined as

$$w = \frac{W}{8\pi k_{\mathrm{c}}},\ \ c_{\mathrm{i}} = C_{\mathrm{i}} R_0,\ \ q = \frac{k_{\mathrm{r}}}{k_{\mathrm{c}}},\ \ \Delta a = \frac{\Delta A}{8\pi R_0 h},$$
$$\overline{\Delta a}_0 = \frac{\overline{\Delta A}_0}{8\pi R_0 h},\ \ \bar{\gamma} = \frac{\gamma R_0^2}{2k_{\mathrm{c}}},\ \ a_{\mathrm{c}} = \frac{A_{\mathrm{c}}}{4\pi R_0^2}. \quad (4)$$

Equilibrium shapes

Equilibrium shapes of erythrocytes in the rouleau correspond to the minimum of their total energy (Eq. 3). Previous theoretical analysis has shown that the energy minima of closed lipid membranes within the ADE model belong to the stationary points of the bending energy (i.e., the first term in Eq. 3) at the constraints of constant a, v, and Δa (Heinrich et al., 1993). Analogously, the equilibrium shapes of erythrocytes in the rouleau can be found among the stationary states of the functional

$$g = \frac{1}{4}\int (c_1 + c_2)^2\, da - \frac{1}{2}\bar{\gamma} a_{\mathrm{c}} - N\Delta a - Mv - La, \quad (5)$$

where N, M, and L are the dimensionless Lagrange multipliers; they represent the difference between the lateral tensions of the membrane leaflets, the pressure difference across the membrane, and the membrane lateral tension, respectively.

A long rouleau composed of identical cells can be assumed to possess an axis of rotational symmetry. Therefore the analysis is restricted to axisymmetric cell shapes and one can make use of the standard approach for axisymmetric parameterization (Svetina and Žekš, 1989; Seifert et al., 1991; Božič et al., 1997). Within this approach, the stationary shapes are determined as follows.

By performing the variation of the functional g one obtains a set of differential equations which define the contour of the cell stationary shape. The shape contour may comprise several distinct sections. The variational procedure also yields the boundary conditions which have to be satisfied at the end points of the contour sections. The differential equations are then solved numerically. In the particular case of an erythrocyte entrapped in a rouleau, the cell contour consists of three distinct sections (Fig. 1): the two membrane parts which are in contact with adjacent cells (the contour from the points A to B and from C to D), and the free part of the membrane (the contour from B to C). Inasmuch as the rouleau is assumed to be composed of identical cells, the cell contour at the contact surfaces can be considered periodic. The analysis shows that at the contact lines of the adhered membranes (points B and C in Fig. 1) the boundary conditions define a discontinuous jump in the membrane contour curvature away from the contact surface (see Appendix A). This change in the curvature is proportional to the square root of the ratio between the adhesion constant and the membrane local bending modulus: $\Delta C_{\mathrm{m}} = \sqrt{\gamma/k_{\mathrm{c}}}$, where ΔC_{m} is the membrane curvature change along the contour (i.e., along the meridian).

There is an analogy between the adhesion of two membranes and the adhesion of a membrane to a flat substrate which was addressed by Seifert and Lipowsky (1990). However, in such a case, the adhesion energy competes with the bending energy of only one membrane, and therefore the change in the curvature at the contact point of a membrane adhering to a flat surface is larger (there, $\Delta C_{\mathrm{m}} = \sqrt{2\gamma/k_{\mathrm{c}}}$; Seifert and Lipowsky, 1990).

Once the stationary shapes of the functional g are obtained, they can be related to the stationary shapes of erythrocytes within the ADE model via relation (Heinrich et al., 1993):

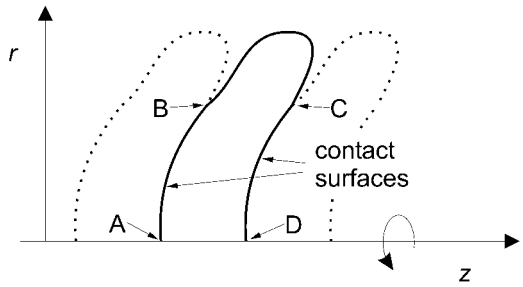

FIGURE 1 Schematic representation of the contour of an erythrocyte in the middle of a long rouleau composed of identical cells. The cell shape is considered to be axisymmetric and to have a periodic boundary condition at the contact surfaces. The points B and C indicate the contact points of the adhering membranes, where the membrane curvature undergoes a discontinuous jump. The dotted contours represent the adhered adjacent cells.

$$N = -2q(\Delta a - \overline{\Delta a_0}). \quad (6)$$

Usually there exist many different stationary erythrocyte shapes at a given set of values of the model parameters v, $\overline{\Delta a_0}$, and $\bar{\gamma}$. They differ in the area difference Δa and in the total energy (Eq. 3). Therefore, the stable equilibrium shape of erythrocytes is finally determined as the stationary shape with the minimal total energy (Appendix B).

THE MODEL PARAMETERS

Within the proposed model, the equilibrium shapes of erythrocytes in the rouleau depend on three free parameters: the relative volume of cells v, the adhesion constant $\bar{\gamma}$, and the effective preferred area difference $\overline{\Delta a_0}$. The fourth model parameter, the ratio between the local and the nonlocal bending moduli, $q = k_t/k_c$, is a material constant of the membrane. Its value is still not precisely known, but both theoretical estimations (Svetina and Žekš, 1996) and experimental data (Hwang and Waugh, 1997) indicate that q of erythrocyte membrane is ~3. Therefore the value of this parameter has been taken to be $q = 3$ in all the calculations in the present analysis.

The simplest of the free model parameters is the relative volume v. In experiments it can be readily estimated from microscope images, and in addition it can be easily regulated by the osmotic properties of the suspending medium. Normal biconcave erythrocytes have $v \approx 0.6$ whereas swollen spherical cells have $v = 1$.

The adhesion constant $\bar{\gamma}$ is a measure of strength of the aggregation forces between erythrocytes. Previous studies found that γ for normal erythrocytes in blood plasma is on the order of 10^{-19} $J/\mu m^2$ (Skalak et al., 1981). Under certain experimental or pathological conditions the adhesion between erythrocytes can be substantially increased. For example, the addition of dextran macromolecules into the suspending medium can produce a more than tenfold increase in the adhesion constant (Chien et al., 1983). Taking into account the value of the erythrocyte local bending modulus ($K_c \approx 2 \times 10^{-19}$ J, Hwang and Waugh, 1997) and the typical surface area of normal erythrocytes ($A \approx 140$ μm^2), the value of the dimensionless adhesion constant $\bar{\gamma}$ is expected to be from ~5 for normal erythrocytes up to 50 and more for the erythrocytes in dextran solution.

The effective preferred area difference $\overline{\Delta a_0}$ is associated with the difference in the number of molecules in the membrane leaflets and the membrane spontaneous curvature. Direct measurements of this parameter are practically impossible, therefore typical experimental values of $\overline{\Delta a_0}$ are not known. Theoretically, a completely relaxed spherical membrane has $\overline{\Delta a_0} = 1$, whereas small $\overline{\Delta a_0}$ encourages membrane invaginations and large $\overline{\Delta a_0}$ promotes evaginations. Erythrocytes possess an active regulation of the membrane lipid asymmetry; therefore it is reasonable to expect that their $\overline{\Delta a_0}$ might change in certain conditions. Also, the preferred area difference of erythrocytes might be affected by certain chemical agents which intercalate selectively into only one of the bilayer leaflets (Sheetz and Singer, 1974).

Furthermore, the morphological changes observed after micropipette aspiration suggest that the erythrocytes might possess a mechanism for relaxation of $\overline{\Delta a_0}$ (Artmann et al., 1997). Such a relaxation would tend to reduce the difference between the lateral tensions of the membrane leaflets N, and accordingly to minimize the membrane nonlocal bending energy (the second term in Eq. 4). A totally relaxed preferred area difference is characterized by $\overline{\Delta a_0} = \Delta a$, and correspondingly $N = 0$. In this case, the ADE model is reduced to the basic bending elasticity model with zero spontaneous curvature, and the equilibrium shapes depend no longer on q and $\overline{\Delta a_0}$.

RESULTS AND DISCUSSION

Equilibrium shapes

The equilibrium shapes of erythrocytes in rouleau have been computed for different values of the model parameters v, $\overline{\Delta a_0}$, and $\bar{\gamma}$. Inasmuch as the mechanisms which control the erythrocyte preferred area difference $\overline{\Delta a_0}$ are not known, the results will be presented for both fixed values of $\overline{\Delta a_0}$ and the totally relaxed $\overline{\Delta a_0}$. In agreement with experimental data and the analysis performed by Skalak et al. (1981), a large number of the determined equilibrium shapes are discoid, i.e., they possess the equatorial mirror symmetry. However, at certain values of the model parameters, the equilibrium shapes lose their mirror symmetry and become cup-shaped. Although this is a novel theoretical result, it is not unexpected inasmuch as the analogous breaking of equatorial mirror symmetry is a well-known feature of free lipid vesicles and free erythrocytes (Svetina and Žekš, 1989).

Two origins of the mirror symmetry breaking can be imagined. The first one is associated with the membrane bending rigidity. At small relative volumes, the rim of the contour of an axisymmetric membrane is highly curved; therefore it is energetically favorable that it occupies as small a part of the membrane surface area as possible. The area of the highly curved region can be reduced if the cell buckles into a cup-like shape and moves the rim toward the axis of rotation. The second origin of the symmetry breaking lies in the double layer nature of the lipid membranes. A large decrease in the preferred area difference of the membrane leaflets eventually leads to membrane invaginations. Consequently, the buckled cup-like shapes become energetically favorable at small $\overline{\Delta a_0}$.

The calculation clearly confirms the expected symmetry behavior of the equilibrium shapes. The mirror symmetric shapes are favorable at large relative volumes and large preferred area differences whereas the asymmetric shapes are favorable at low v and small $\overline{\Delta a_0}$. The effects of changing v and $\overline{\Delta a_0}$ on the equilibrium shapes are presented in Fig. 2, *A* and *B*. For example, at $\bar{\gamma} = 20$, and $\overline{\Delta a_0} = 1$, a decrease of the relative volume from $v = 0.45$ to $v = 0.35$ breaks the mirror symmetry and the cell becomes visibly invaginated (Fig. 2 *A*). Similarly, the mirror symmetry of the equilibrium shape is broken if the preferred area difference $\overline{\Delta a_0}$ is decreased (Fig. 2 *B*).

The effect of the adhesion constant $\bar{\gamma}$ on the equilibrium shapes is presented in Fig. 2 *C*. Here, large adhesion strengths tend to maximize the area of the contact surface between the cells. Thus, an increasing adhesion constant $\bar{\gamma}$ flattens the cell and encourages the discoid shapes (Fig. 2 *C*).

Because the equilibrium erythrocyte shapes depend on the three free model parameters v, $\bar{\gamma}$, and $\overline{\Delta a_0}$, the regions of the discoid and the cup-like shapes lie in a three-dimensional phase diagram. The three-dimensional phase diagram can be conveniently presented in the form of the projections on the planes $v - \bar{\gamma}$ (Fig. 3) and $\overline{\Delta a_0} - \bar{\gamma}$ (Fig. 4), which show the lines of the symmetry breaking, i.e., the lines that delimit the regions of the discoid and the cup-like shapes.

The lines on the boundary between the discoid and the cup-like shapes in the $v - \bar{\gamma}$ plane at constant values of $\overline{\Delta a_0}$ are presented in Fig. 3. The cup-like shapes lie below the

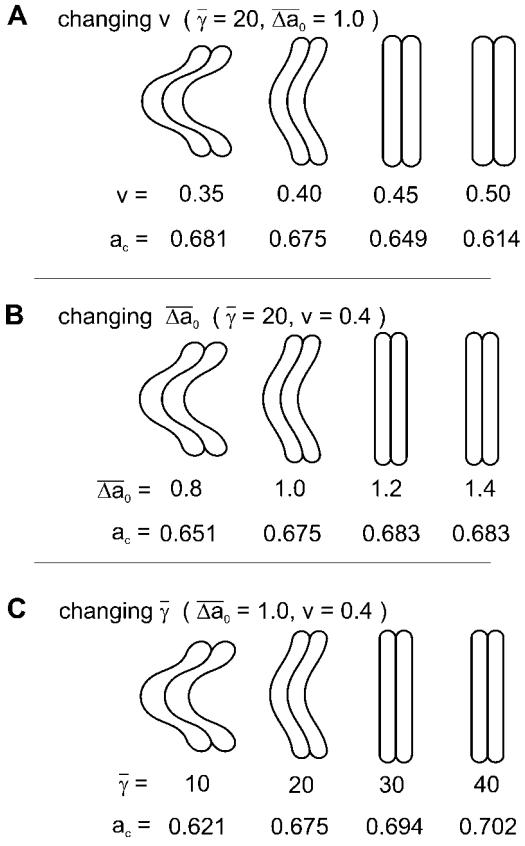

FIGURE 2 Equilibrium shapes of erythrocytes in a long rouleau calculated at different values of the model parameters. Two adjacent cells are represented in each case. The axis of symmetry is horizontal in all cases. Note that the equilibrium shapes are either discoid or cup-shaped. The corresponding relative areas of the contact surface a_c are also given. (*A*) The dependence on the relative volume υ at constant $\bar{\gamma} = 20$ and $\overline{\Delta a_0} = 1.0$; (*B*) The dependence on the effective preferred area difference $\overline{\Delta a_0}$ at constant $\bar{\gamma} = 20$ and $\upsilon = 0.4$; and (*C*) The dependence on the adhesion constant $\bar{\gamma}$ at constant $\overline{\Delta a_0} = 1.0$ and $\upsilon = 0.4$.

symmetry breaking lines at small values of υ and $\bar{\gamma}$, and the discoid shapes are above the lines. Clearly, the cup-like shapes are favored at small υ, $\bar{\gamma}$, and $\overline{\Delta a_0}$. The dashed line in Fig. 3 represents the line of symmetry breaking in the case of a totally relaxed preferred area difference $\overline{\Delta a_0}$. Note that in this case, the equilibrium shapes do not depend on $\overline{\Delta a_0}$. The values of Δa for the shapes along this dashed line are $\sim$1.1.

The lines of the symmetry breaking in the case of changing $\overline{\Delta a_0}$ and $\bar{\gamma}$ at constant values of the relative volume are presented in Fig. 4. The region of cup-like shapes is below the lines at small values of $\overline{\Delta a_0}$ and $\bar{\gamma}$. Clearly, at smaller volumes the line of the symmetry breaking is moved toward larger values of $\overline{\Delta a_0}$ and $\bar{\gamma}$.

The type of the transition between the discoid and the cup-like shapes across the symmetry breaking lines can be determined from a detailed analysis of the stationary shapes (see Appendix B). The following results have been found. In the case of a fixed $\overline{\Delta a_0}$ and the expected values of q (*solid lines* in Figs. 3 and 4), all the transitions between the discoid and the cup-like shapes are continuous. In the case of the totally relaxed $\overline{\Delta a_0}$ (*dashed line* in Fig. 3), the transitions are continuous only above $\bar{\gamma} \approx 10$. Nevertheless, even in the case of the discontinuous transitions below $\bar{\gamma} \approx 10$, the energy barrier between the symmetric and nonsymmetric shapes is of the order of only several kT per cell, and the discontinuity is not likely to be observable in experiments.

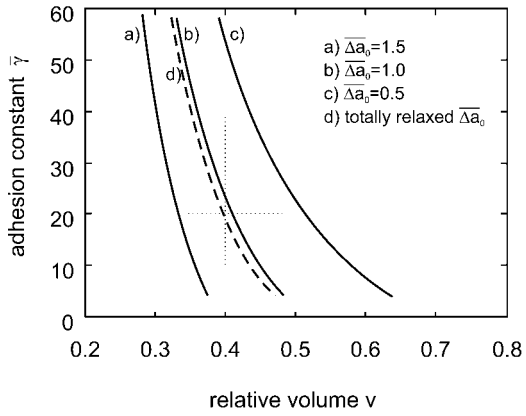

FIGURE 3 The lines which delimit the region of the discoid equilibrium erythrocyte shapes from the region of the cup-like shapes in the plane $\upsilon - \bar{\gamma}$. The solid lines represent the situations at three different constant values of $\overline{\Delta a_0}$. The discoid shapes lie above the delimiting lines (at large $\bar{\gamma}$ or υ) and the cup-like shapes are in the region below the lines (at small $\bar{\gamma}$ and υ). All the transitions between the discoid and the cup-like shapes across these lines are continuous. The dashed line represents the delimiting values of $\bar{\gamma}$ and υ in the case of the totally relaxed $\overline{\Delta a_0}$. The dotted lines represent the paths containing the shapes presented in Fig. 2, *A* and *C*.

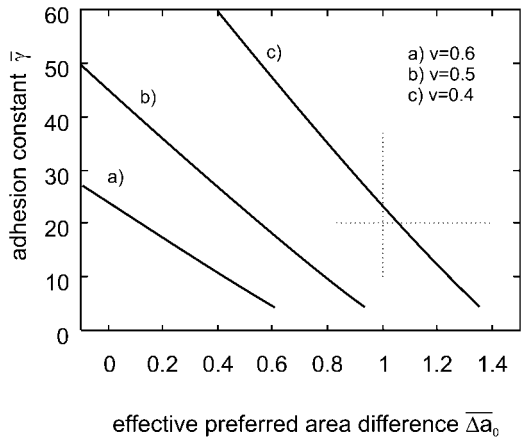

FIGURE 4 The lines which delimit the region of the discoid equilibrium erythrocyte shapes from the region of the cup-like shapes in the plane $\overline{\Delta a_0} - \bar{\gamma}$. The solid lines represent the situations at three different constant values of υ. The discoid equilibrium shapes lie above the delimiting lines (at large $\bar{\gamma}$ or $\overline{\Delta a_0}$) and the cup-like equilibrium shapes are in the region below the lines (at small $\bar{\gamma}$ and $\overline{\Delta a_0}$). All the transitions between the discoid and the cup-like shapes across these lines are continuous. The dotted lines represent the paths containing the shapes presented in Fig. 2, *B* and *C*.

Model validity

At very small values of the adhesion constant $\bar{\gamma}$, the free erythrocytes can aggregate only if their deformations are small. Presumably, the shapes of erythrocytes in such aggregates would be far from the shapes assumed by the presented model. The situation at small adhesion constants is therefore not properly addressed by the present analysis. The comparison of the energies of free erythrocytes and adhered erythrocytes within our model revealed that the rouleau formation is energetically favorable only at the adhesion constants $\bar{\gamma}$ larger than ~4. This was the reason for not showing the symmetry breaking lines at small adhesion constants in Figs. 3 and 4.

In the limit of very large adhesion constant, the equilibrium shapes of aggregated erythrocytes at a given relative volume have maximized contact surface area. In the case of a formed long rouleau, these limit shapes are cylindrical. However, the aggregation process at large adhesion constants does not lead to a long cylindrical rouleau. Namely, when erythrocytes are aggregating at large adhesion strength, they first form nonaxisymmetrical spherical doublets, which maximize the two-cell system contact surface area (Tilley et al., 1987). Adhesion of additional cells to such spherical doublets leads to irregular erythrocyte aggregates, which are not described by the presented model.

Relation to free erythrocytes

An informative comparison between the results of the present study and those obtained for free erythrocytes can be obtained using the relation between the relative volume v and the area difference Δa for stationary shapes at $N = 0$. Fig. 5 shows this relation in the case of free erythrocytes and aggregated erythrocytes at two different adhesion constants. The solid lines represent the cup-like shapes and the dashed lines represent the discoid shapes. Note that the dashed lines corresponding to the two examples of aggregated erythrocytes practically coincide. At small values of Δa, the solid lines representing aggregated erythrocytes end where the cell membrane touches itself from the inside of the cell and the presented model loses validity. At large relative volumes, both free and aggregated erythrocytes exist only in discoid shapes. Inasmuch as the adhesion unbends the invaginations at the cell poles, the aggregated erythrocytes have larger Δa than the corresponding free cells. Apparently, the increasing adhesion strength pushes the solutions of the stationary cup-like shapes toward smaller volumes.

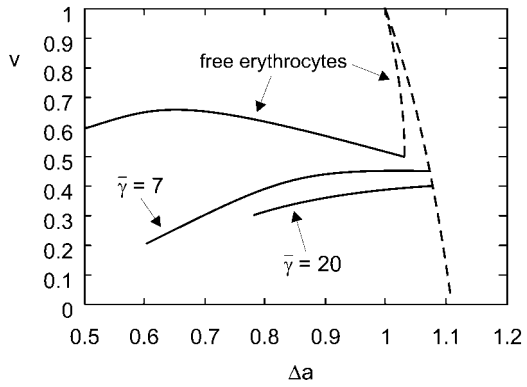

FIGURE 5 The relation between the relative volume v and the dimensionless area difference Δa for the stationary shapes at $N = 0$. The relation is presented for free erythrocytes and for aggregated erythrocytes at two values of the adhesion constant $\bar{\gamma}$. The solid and the dashed lines represent the cup-like shapes and the mirror symmetric shapes, respectively.

CONCLUSIONS

In the present paper we theoretically analyze the equilibrium shapes of erythrocytes in rouleau formation. The analysis takes into account the mechanical properties of the erythrocyte lipid membrane, described by the ADE model, and the strength of the adhesion between adjacent cells. An important step in the analysis is the proper description of the adhesion of curved axisymmetric membranes and the calculation of the membrane curvature discontinuity at the points of the membrane contact.

The results predict that the erythrocytes in the rouleau can have either a discoid or a cup-like shape (Fig. 2). The shapes of aggregated erythrocytes depend on three parameters: the erythrocyte relative volume v, the effective preferred area difference $\overline{\Delta a_0}$, and the relative adhesion constant $\bar{\gamma}$. In general, the discoid shapes are favored at larger v, $\overline{\Delta a_0}$, and $\bar{\gamma}$, whereas at low values of these parameters the rouleau is expected to consist of cup-shaped erythrocytes (Figs. 3 and 4). The two shape classes of aggregated erythrocytes and their dependence on the relative volume and the effective preferred area difference are analogous to the behavior of discoid and stomatocyte shapes of free erythrocytes. Note that the effective preferred area difference $\overline{\Delta a_0}$ is a combination of the preferred area difference between the bilayer leaflets ΔA_0 and the membrane spontaneous curvature C_0. Inasmuch as the mechanisms of the regulation of $\overline{\Delta a_0}$ in erythrocytes are not well established, the results were presented at different fixed values of $\overline{\Delta a_0}$, as well as for a totally relaxed $\overline{\Delta a_0}$.

Although the proposed analysis is simplified by considering only very long rouleaux composed of identical erythrocytes, it can qualitatively predict the behavior of experimentally observable rouleaux composed of a finite number of nonuniform cells. In fact, if the model involved the possible nonuniformity of the adhered cells, the number of the model parameters would increase significantly and any general presentation of its theoretical predictions would be impossible.

The predicted transitions between the discoid and the cup-like shapes of erythrocytes in a rouleau can be very

interesting from the experimental point of view. Namely, inasmuch as the symmetry properties can be readily determined experimentally, the presented analysis can provide a useful framework for systematic studies of erythrocyte membrane mechanical properties and intercellular adhesion. It would be particularly instructive to study the effect of various stomatocytogenic and echinocytogenic agents on erythrocyte shape in the rouleau.

Finally, the analysis can be easily extended in at least two ways. For example, a similar analysis can be developed for quantitative interpretation of experiments involving only a small number of adhered cells. In addition, the theory can be extended to describe the adhesion of two membranes possessing different local bending moduli, which could be useful in the studies of impaired erythrocytes or multilamellar lipid vesicles.

APPENDIX A: BOUNDARY CONDITIONS

A general treatment of the boundary conditions of stationary axisymmetric membrane shapes has been extensively described elsewhere (see, for example, Jülicher and Seifert, 1994); therefore, here we will focus only on the treatment of the adhesion of curved membranes, and on the boundary conditions at the points of membrane contact (points B and C in Fig. 1).

The parameterization of a closed axisymmetric surface can be conveniently performed via coordinates $r(s)$ and $\psi(s)$, where r is the radial distance of the surface contour to the axis of symmetry, ψ is the angle between the symmetry axis and the contour normal, and s is the arc length along the contour. In the case of a long rouleau of identical cells, the membrane shape along the contact area can be considered identical on both sides of the cell (Fig. 1). Therefore, the contour from point A to point B coincides with the contour from point D to point C, and the integrations along these contours can be joined into a single one. By using the relations $v = (3/4)\int r^2 \sin\psi\, ds$, and $a = (1/2)\int r\, ds$, the functional g (Eq. 5) can thus be written as

$$g = \int_A^B \mathcal{L}_c\, ds + \int_B^C \mathcal{L}_f\, ds, \tag{7}$$

where $\mathcal{L}_c$ is the combined Lagrange function for the two membrane parts which are in contact:

$$\mathcal{L}_c = \frac{1}{4} r \left(\frac{\sin\psi}{r} + \dot{\psi}\right)^2 + \left(L - \frac{1}{2}\bar{\gamma}\right) r + 2\Gamma(\dot{r} - \cos\psi), \tag{8}$$

and $\mathcal{L}_f$ is the Lagrange function for the free part of the membrane:

$$\mathcal{L}_f = \frac{1}{8} r \left(\frac{\sin\psi}{r} + \dot{\psi}\right)^2 + \frac{1}{2} Lr - \frac{3}{4} Mr^2 \sin\psi - \frac{1}{4} rN \left(\frac{\sin\psi}{r} + \dot{\psi}\right) + \Gamma(\dot{r} - \cos\psi). \tag{9}$$

We took into consideration that the membrane curvature along the meridians c_m equals $\dot{\psi}$ and the membrane curvature along the parallels c_p is $\sin\psi/r$. The additional Lagrange multiplier $\Gamma(s)$ had to be introduced because the variables $r(s)$ and $\psi(s)$ are related via $\dot{r} = dr/ds = \cos\psi$. Note that in the Lagrangian $\mathcal{L}_c$, the terms containing M and N have been canceled out whereas the terms with L and the bending energy have been doubled.

The analysis can be carried out in a concise way by using the Hamilton notation. Within this approach, one defines the vector of variables $\mathbf{x} = (r, \psi, \Gamma)$, and a generalized momentum, $\mathbf{p} = (\partial\mathcal{L}/\partial\dot{r}, \partial\mathcal{L}/\partial\dot{\psi}, \partial\mathcal{L}/\partial\dot{\Gamma})$. The generalized momentum in the case of the membrane in contact is $\mathbf{p}_c = (2\Gamma, (1/2)r(\sin\psi/r + \dot{\psi}), 0)$ and in the case of the free membrane $\mathbf{p}_f = (\Gamma, (1/4)r(\sin\psi/r + \dot{\psi} - N), 0)$. The corresponding Hamiltonians ($\mathcal{H} = -\mathcal{L} + \dot{\mathbf{x}} \cdot \mathbf{p}$) are:

$$\mathcal{H}_c = \frac{1}{4} r \left(\dot{\psi}^2 - \frac{\sin^2\psi}{r^2}\right) + \left(\frac{1}{2}\bar{\gamma} - L\right) r + 2\Gamma\cos\psi \tag{10}$$

$$\mathcal{H}_f = \frac{1}{8} r \left(\dot{\psi}^2 - \frac{\sin^2\psi}{r^2}\right) + \frac{3}{4} Mr^2 \sin\psi - \frac{1}{2} Lr + \frac{1}{4} N \sin\psi + \Gamma\cos\psi \tag{11}$$

According to the theory of the calculus of variations, the stationary contour has to satisfy the boundary conditions

$$[\mathcal{H}_c \delta s - \mathbf{p}_c \cdot \delta\mathbf{x}]_A^B + [\mathcal{H}_f \delta s - \mathbf{p}_f \cdot \delta\mathbf{x}]_B^C = 0 \tag{12}$$

At the points B and C, the variations δs, δr, and $\delta\psi$ are arbitrary. Nevertheless, because of the periodic contact surface they are not independent but are related via $\delta s_c|_B = \delta s_f|_B = -\delta s_f|_C$, $\delta r_c|_B = \delta r_f|_B = \delta r_f|_C$, and $\delta\psi_c|_B = \delta\psi_f|_B = \delta\psi_f|_C$. Therefore the boundary conditions (Eq. 12) at the points B and C give a set of three equations:

$$4\bar{\gamma} + 2\dot{\psi}_c^2|_B - \dot{\psi}_f^2|_B - \dot{\psi}_f^2|_C = 0 \tag{13}$$

$$2\Gamma_c|_B - \Gamma_f|_B + \Gamma_f|_C = 0 \tag{14}$$

$$2\dot{\psi}_c|_B - \dot{\psi}_f|_B + \dot{\psi}_f|_C = 0 \tag{15}$$

Combining Eqs. 13 and 15 yields

$$\dot{\psi}_f|_B = \dot{\psi}_c|_B + \sqrt{2\bar{\gamma}} \tag{16}$$

$$\dot{\psi}_f|_C = -\dot{\psi}_c|_B + \sqrt{2\bar{\gamma}} \tag{17}$$

Thus, the change in curvature at the points B and C equals $\Delta c_m = \sqrt{2\bar{\gamma}}$.

APPENDIX B: DETAILED ANALYSIS OF THE STATIONARY SHAPES

A detailed analysis of the stationary shapes of the functional g (Eq. 5) will be presented for the case of the cup-like and the discoid shapes. At fixed values of v and $\bar{\gamma}$, the stationary shapes of the functional g differ in the area difference Δa, and correspondingly in the difference between the lateral tensions of the bilayer leaflets N. As an example, we analyze the relation between N and Δa for the stationary shapes for $v = 0.45$ and $\bar{\gamma} = 7$ (Fig. 6 *A*). Note that the stationary shapes of the functional g do not depend on the parameters $\overline{\Delta a_0}$ and q. The solid and the dashed line in Fig. 6 *A* represent the cup-like shapes and the discoid shapes, respectively.

The case of a totally relaxed preferred area difference $\overline{\Delta a_0}$ is characterized by the zero difference between the lateral tensions of the bilayer leaflets, $N = 0$. In Fig. 6 *A*, there are three solutions with $N = 0$, one with the discoid and two with the cup-like shapes. The stability of the three solutions can be determined from the total energy of the stationary shapes, which is presented in Fig. 6 *B*. Note that in the case of a totally relaxed $\overline{\Delta a_0}$ the nonlocal bending energy equals zero, and the total energy is the sum of the bending and the adhesion energy only. As it turns out, the cup-like stationary shape at $\Delta a \approx 1.045$ is, in fact, in the energy maximum and is thus

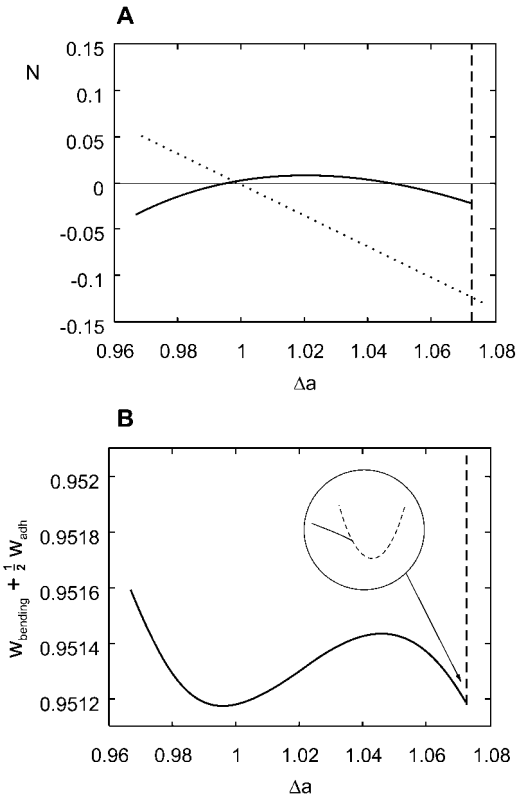

FIGURE 6 (*A*) The relation between the difference between the lateral tensions of the bilayer leaflets N and the area difference Δa for the stationary shapes at $\upsilon = 0.45$ and $\bar{\gamma} = 7$. The solid and the dashed lines represent the cup-shaped and the discoid stationary shapes respectively. The dashed line has a steep positive slope. The dotted line represents $N = -2q(\Delta a - \overline{\Delta a_0})$ for $q = 3$ and $\overline{\Delta a_0} = 1.0$; (*B*) The energies of the stationary shapes presented in *A*. The dashed line is a steep parabola.

unstable. The other two stationary shapes are stable and have the same energy because the point with $\upsilon = 0.45$ and $\bar{\gamma} = 7$ lies on the symmetry breaking line for the case $N = 0$. Inasmuch as the stable discoid and the stable cup-like shapes differ significantly in Δa, the transition between them is discontinuous.

In the case of a fixed effective preferred area difference $\overline{\Delta a_0}$, the equilibrium shapes are related to stationary shapes of the functional g via Eq. 6. The solutions of this equation can be conveniently presented graphically as the intersections of the function $N(\Delta a)$ and the line representing the line $N = -2q(\Delta a - \overline{\Delta a_0})$. The dotted line in Fig. 6 *A* is such a representation for the values $q = 3$ and $\overline{\Delta a_0} = 1$. It can be seen that in this case, there are two intersections and correspondingly two solutions for the equilibrium shapes, one with the symmetric shapes and the other with the nonsymmetric shapes. The calculation of the total energy of these two shapes reveals that the cup-like shape is the one with the smallest energy and is thus in the stable equilibrium (the total energy at fixed $\overline{\Delta a_0}$ can be viewed as the sum of the energy presented in Fig. 6 *B* and a parabola $q(\Delta a - \overline{\Delta a_0})^2$). Fig. 6 *A* also shows that at high $\overline{\Delta a_0}$, there would be no intersections of the dotted line with the nonsymmetric shapes and the equilibrium shapes would have to be symmetric. Note that the value of q does not qualitatively affect the system behavior as long as $2q$ is larger than the slope $dN/d\Delta a$ at the point where $N(\Delta a)$ of the cup-like shapes approaches $N(\Delta a)$ of the discoid shapes.

REFERENCES

Artmann, G. M., K.-L. Sung, T. Horn, D. Whittemore, G. Norwich, and S. Chien. 1997. Micropipette aspiration of human erythrocytes induces echinocytes via membrane phospholipid translocation. *Biophys. J.* 72:1434–1441.

Barshtein, G., I. Tamir, and S. Yedgar. 1998. Red blood cell Rouleaux formation in dextran solution: dependence on polymer conformation. *Eur. Biophys. J.* 27:177–181.

Bishop, J. J., P. R. Nance, A. S. Popel, M. Intaglietta, and P. C. Johnson. 2001. Effect of erythrocyte aggregation on velocity profiles in venules. *Am. J. Physiol. Heart Circ. Physiol.* 280:H222–H236.

Božič, B., S. Svetina, B. Žekš, and R. E. Waugh. 1992. Role of lamellar membrane structure in tether formation from bilayer vesicles. *Biophys. J.* 61:963–973.

Božič, B., S. Svetina, and B. Žekš. 1997. Theoretical analysis of the formation of membrane microtubes on axially strained vesicles. *Phys. Rev. E.* 55:5834–5842.

Candiloros, H., S. Muller, O. Ziegler, M. Donner, and P. Drouin. 1996. Role of albumin glycation on the erythrocyte aggregation: an in vitro study. *Diabetic Med.* 13:646–650.

Chien, S., L. A. Sung, S. Simchon, M. M. Lee, K.-M. Jan, and R. Skalak. 1983. Energy balance in red cell interactions. *Ann. N. Y. Acad. Sci.* 416:190–206.

Darmani, H., and W. T. Coakley. 1990. Membrane membrane interactions—parallel membranes or patterned discrete contacts. *Biochim. Biophys. Acta.* 1021:182–190.

Heinrich, V., S. Svetina, and B. Žekš. 1993. Nonaxisymmetric vesicle shapes in a generalized bilayer-couple model and the transition between oblate and prolate axisymmetric shapes. *Phys. Rev. E.* 48:3112–3123.

Hwang, W. C., and R. E. Waugh. 1997. Energy of dissociation of lipid bilayer from the membrane skeleton of red blood cells. *Biophys. J.* 72:2669–2678.

Jülicher, F., and U. Seifert. 1994. Shape equations for axisymmetric vesicles: a clarification. *Phys. Rev. E.* 49:4728–4731.

Miao, L., U. Seifert, M. Wortis, and H. G. Döbereiner. 1994. Budding transitions of fluid-bilayer vesicles—the effect of area-difference elasticity. *Phys. Rev. E.* 49:5389–5407.

Seifert, U., and R. Lipowsky. 1990. Adhesion of vesicles. *Phys. Rev. A.* 42:4768–4771.

Seifert, U., K. Berndl, and R. Lipowsky. 1991. Shape transformations of vesicles: phase diagram for spontaneous-curvature and bilayer-coupling models. *Phys. Rev. A.* 44:1182–1202.

Sheetz, M. P., and S. J. Singer. 1974. Biological membranes as bilayer couples. A molecular mechanism of drug-erythrocyte interactions. *Proc. Natl. Acad. Sci. USA.* 71:4457–4461.

Skalak, R., P. R. Zarda, K.-M. Jan, and S. Chien. 1981. Mechanics of Rouleau formation. *Biophys. J.* 35:771–781.

Skalak, R., and S. Chien. 1983. Theoretical-models of Rouleau formation and disaggregation. *Ann. N. Y. Acad. Sci.* 416:138–148.

Svetina, S., M. Brumen, and B. Žekš. 1985. Lipid bilayer elasticity and the bilayer couple interpretation of red cell shape transformations and lysis. *Stud. Biophys.* 110:177–184.

Svetina, S., and B. Žekš. 1989. Membrane bending energy and shape determination of phospholipid vesicles and red blood cells. *Eur. Biophys. J.* 17:101–111.

Svetina, S., and B. Žekš. 1996. Elastic properties of closed bilayer membranes and the shapes of giant phospholipid vesicles. *In* Handbook of Nonmedical Applications of Liposomes. D. D. Lasic, and Y. Barenholz, editors. CRC Press, Boca Raton, FL. 13–42.

Tilley, D., W. T. Coakley, R. K. Gould, S. E. Payne, and L. A. Hewison. 1987. Real time observations of polylysine, dextran and polyethylene glycol induced mutual adhesion of erythrocytes held in suspension in an ultrasonic standing wave field. *Eur. Biophys. J.* 14:499–507.